



## **Assessment of fetal left atrial volume and function using a novel left atrial volume tracking method**

**Authors:** Xiaohui Peng, Suping Zhou, Jiaoni Wang, Mei Pan, Bei Wang, Xiaolu Sun, Bowen  
Zhao

**Article type:** Original article

**Received:** May 20, 2022

**Accepted:** October 10, 2022

**Early publication date:** October 24, 2022

This article is available in open access under Creative Common Attribution-Non-Commercial-No Derivatives 4.0 International (CC BY-NC-ND 4.0) license, allowing to download articles and share them with others as long as they credit the authors and the publisher, but without permission to change them in any way or use them commercially.

# **Assessment of fetal left atrial volume and function using a novel left atrial volume tracking method**

**Short title:** A novel left atrial volume tracking method

Xiaohui Peng<sup>1</sup>, Suping Zhou<sup>2</sup>, Jiaoni Wang<sup>1</sup>, Mei Pan<sup>1</sup>, Bei Wang<sup>1</sup>, Xiaolu Sun<sup>1</sup>, Bowen Zhao<sup>1</sup>

<sup>1</sup>Department of Diagnostic Ultrasound and Echocardiography, Sir Run Run Shaw Hospital, Zhejiang University Medical College, Hangzhou, China

<sup>2</sup>Department of Diagnostic Ultrasound, Peking University Shenzhen Hospital, Shenzhen, China

## **Correspondence to:**

Bowen Zhao, MD,

Department of Diagnostic Ultrasound and Echocardiography,

Sir Run Run Shaw Hospital, Zhejiang University Medical College,

3 Qingchun Road East, Hangzhou,

Zhejiang Province, People's Republic of China,

phone: +86 571 86 006 331,

e-mail: zbwcjp@zju.edu.cn

**WHAT'S NEW?**

In adults, 2-dimensional echocardiography (2DE) biplane Simpson's method was recommended by American Society of Echocardiography to evaluate left atrial volume (LAV) and the accuracy has been validated in vitro models and angiography. This study applies a new left atrial volume tracking (LAVT) method, which is based on Simpson's rule algorithm, to establish normal values for human LAV during the second half of gestation. LAVT method has proven to be a feasible method to estimate fetal LAV as well as left atrial ejection fraction (EF) during the second half of gestation, suggesting the potential value of this method in assessing left ventricular diastolic function of fetal hearts, especially under pathological conditions in mater or in fetus.

## **ABSTRACT**

**Background:** A number of fetal cardiovascular structural defects may alter the hemodynamics of the cardiac chambers resulting in changes in chamber sizes. Quantitative measurements of the sizes of cardiac chambers can augment the diagnostic power of fetal echocardiography.

**Aims:** Using a new left atrial volume tracking (LAVT) method, time-left atrial volume curves (TLAVCs) can be automatically obtained. The goal of this study was to examine whether this method can be used to evaluate left atrial volume (LAV) and provide reference values for LAV, and indices of left atrial function in normal human fetuses.

**Methods:** 204 normal human fetuses were enrolled. Using LAVT, the maximal left atrial volume (LAV<sub>max</sub>) and minimal left atrial volume (LAV<sub>min</sub>) were measured from TLAVCs. Left atrial ejection fraction (EF) was calculated. The maximal left atrial area (LAA<sub>max</sub>) and minimal left atrial area (LAA<sub>min</sub>) were measured using manual method tracing.

**Results:** From 21–40 weeks, mean LAV<sub>max</sub> increased from 0.27 ml to 4.15 ml and mean LAV<sub>min</sub> increased from 0.13ml to 2.26ml, respectively. While the EF remained stable at around 0.43. From 21–40 weeks, mean LAA<sub>max</sub> increased from 0.61 cm<sup>2</sup> to 2.64 cm<sup>2</sup> and mean LAA<sub>min</sub> increased from 0.34 cm<sup>2</sup> to 1.53 cm<sup>2</sup>.

**Conclusions:** This study establishes reference values for fetal LAV during the second half of gestation. LAVT method has proven to be a feasible method to estimate fetal LAV, suggesting the potential value in assessing left atrial function.

**Key words:** left atrial tracking, fetal echocardiography, left atrial volume.

## **INTRODUCTION**

Fetal echocardiography has become a reliable technique for assessing structural defects and arrhythmias in the second and the third trimesters of gestation [1–2]. A number of fetal cardiovascular structural defects as well as arrhythmias may alter the hemodynamics of the atrial and/or ventricular chambers resulting in changes in chamber sizes [3–6]. The size and shape of chamber in fetus are related with the perinatal death [7]. Quantitative measurements of the sizes of cardiac chambers may enable the physician to penetrate the growth pattern of normal fetal hearts and augment the diagnostic power of fetal echocardiography. Traditional methods include measurements of the diameters of cardiac chambers by M-mode and 2-dimensional echocardiography (2DE) methods [8–9]. Chamber volume calculation from 2DE does not rely on measuring a single dimension, but rather covers the entire cross-sectional area of the chamber; therefore, measurements using 2DE may better estimate volume changes. The accuracy of ventricular volume determination by 2DE using a biplane Simpson's rule algorithm was firstly been proved in fetal sheep [10], and then this method was further used in normal human fetuses [11]. In adults, 2DE biplane Simpson's method was recommended by American Society of Echocardiography to evaluate left atrial volume (LAV) and the accuracy has been validated in vitro models and angiography [12–14]. Left atrial volume tracking (LAVT) method is a newly developed method, which is an automated measurement and is evaluated in images based on off-line analysis and might be useful for measuring LAV curves precisely in adults [15]. Recently, it has also been previously used in fetal hearts [16–17]. In our study, we apply this method, which is based on Simpson's rule algorithm, to establish normal values for human LAV during the second half of gestation.

## **METHODS**

### **Study population**

The study population consisted of singleton pregnancies from 21 to 40 weeks' gestation undergoing fetal echocardiography scans at the Sir Run Run Shaw Hospital, Zhejiang University College of Medicine in Hangzhou, China. This study was approved by the Ethics Committee of the Sir Run Run Shaw Hospital and informed consents were obtained from all participants. Inclusion criteria were: accurate gestational age (GA) based upon measurement of the fetal biparietal diameter (BPD) and femoral length; normal fetal growth, absence of medical complications, such as diabetes mellitus, hypertension. The exclusion criteria were as follows: fetal cardiac and extracardiac abnormalities; abnormal intrauterine fetal growth; inability to obtain a standard view due to variable fetal position.

A total of 204 fetuses had normal cardiac morphology and normal sinus rhythm in the second and third trimesters were used as the research objects. Inspection of the atrial symmetry would firstly be made on a standard four-chamber heart view. If there was any asymmetry in atrial size, we would measure the width and length of the left and right atrium and then calculate the width ratio of left and right atrium (RA/LA width ratio); if the RA/LA width ratio was in the range of 0.8~1.2, the fetus was regarded as having normal atrial morphology.

### **The principles of the left atrial volume tracking method**

The LAVT method uses adaptive density gradient (ADG) method with the ability of automatic construction of the LAV profile applying 2-dimensional tissue tracking technique. In the ADG method [18], only the pixels on the sector beam which has the necessary information for tracking process would be tracked, resulting in reducing the number of pixels for tracking and saving tracking time (Supplementary material, *Video S1*). Therefore, the ADG method can produce faster calculation speed, higher accuracy, and higher frame rates compared to the conventional block matching method [18]. Image clip of the apical 4-chamber view in one cardiac cycle was stored into the commercially available EUB-900 ultrasound scanner (Hitachi Medical Corporation, Chiba, Japan). The automatic construction of the left atrial curve has been performed off-line using a prototype viewer (Hitachi Medical Corporation, Chiba, Japan). Left atrial endocardium was manually traced at first, and subsequent LAV at each frame was automatically calculated by the

single plane Simpson's rule, resulting in the construction of the LAV curve within one minute. The biplane Simpson's rule can also be applied in this procedure.

## **Echocardiography**

Echocardiographic examinations were performed on the subjects with a Philips iE33 xMATRIX ultrasound system (Philips Medical System, Bothell, WA, USA) with a 1.0–5.0 or 3.0–8.0MHz transducer. General schematic sonographic examination was performed to rule out fetal abnormalities and was followed by detailed fetal 2-dimensional and color Doppler echocardiography to exclude fetal heart anomalies [19]. The maximal left atrial area (LAA<sub>max</sub>) and minimal left atrial area (LAA<sub>min</sub>) were traced from the 4-chamber view. We magnified the images to minimize calibration induced measurement errors. Then, we used the commercially available EUB-900 ultrasound scanner (Hitachi Medical Corporation, Chiba, Japan) to obtain TLAVCs. The fetal left atrium was imaged in orthogonal planes corresponding to those obtained postnatally for volume calculation equivalent to apical 4- and 2-chamber views. Imaging of the left atrium was considered satisfactory if all 4 chambers, the left ventricular apex, both atrioventricular valves and confluence of pulmonary veins were seen in the 4-chamber view. The display of the mitral valve, apex, and aortic valve served as coordinates in the 2-chamber view. After optimizing the gain, dynamic range, and sensitivity time control, images were digitally recorded for 2 seconds (about 5 to 6 cardiac cycles), stored on hard discs for later analysis. Then, left atrial endocardium of the apical 4-chamber and 2-chamber view was manually traced at first frame. This measurement was based on the innermost bright edge convention, which disregarded the orifices of the pulmonary veins but not the floating foramen ovale flap. Subsequently, LAV at each frame was automatically calculated by the single plane and biplane Simpson's rule. Finally, TLAVCs were automatically obtained (**Figure 1**). The LAV<sub>max</sub> and LAV<sub>min</sub> were measured from the volume waveform by biplane Simpson's rule. Calculations were made in 3 to 6 consecutive cardiac cycles and averaged. Left atrial EF was calculated as the difference between LAV<sub>max</sub> and LAV<sub>min</sub>, divided by end-diastolic volume. In 20 randomly selected fetuses, both LAV<sub>max</sub> and LAV<sub>min</sub> were measured by the same observer (B.W.Z) twice as well as another observer (SPZ) in order to compare the measurements and to calculate interobserver and interobserver agreement.

## Statistical analysis

For each variable, a simple scatter plot graph was firstly obtained to observe roughly their correlations and tendency with GA. Regression analysis was used to examine the correlation between measured volumes and GA, and measured volumes and BPD. Separate linear, quadratic, cubic and logarithmic regression models were fitted to identify the optimal one. Based on the equations acquired for both the mean and the SD, population reference intervals for gestational age were estimated. Bland–Altman analysis was used to compare the measurement agreement and bias for a single observer and two observers [20–21].  $P < 0.05$  was considered statistically significant. The data were analyzed using Excel for Windows 2003 (Microsoft Corp., Redmond, WA, USA) and IBM SPSS package 22.0 (SPSS, Inc., Chicago, IL, US).

## RESULTS

Of all the 204 fetuses, 17 fetuses were excluded because of inadequate imaging. Optimal TLAVCs were acquired in the rest 187 fetuses (success rate was 92%). Limiting factors for TLAVCs acquisition included: low image resolution at young GA, abundant fetal movement, numerous acoustic shadows, and a persistent unfavorable fetal position. It was found that all the target volumes correlated strongly both with gestational age and BPD. The best-fitted regression equations of the mean of the studied parameters against GA and BPD are shown in Supplementary material, *Table S1*. The curves of best fit for mean LAVmax and LAVmin against both the GA (**Figure 2**) and BPD (**Figure 3**) as the independent variable were the quadratic curve. Meanwhile, the best model for mean LAAMax and LAAMin based on GA was a linear regression. Based on the acquired equations the predicted mean LAVmax ranged from 0.27 ml at 21 weeks to 4.15 ml at 40 weeks, and the mean LAVmin ranged from 0.13mL at 21 weeks to 2.26 ml at 40 weeks. **Figure 4** demonstrated the increase in LAAMax and LAAMin with advancing GA. The detailed values are shown in Supplementary material, *Table S2*. Meanwhile, pearson correlation analysis showed there was no significant correlation between mean left atrial EF and GA, and it remained fairly stable at around 0.43 with advancing GA (**Figure 2**). Bland-Altman analysis showed that there was a good agreement of the LAV data between two

observers and for a single observer. The intraobserver variation coefficient for measured mean LAVmax and LAVmin was 5.0%, 6.6%, respectively; and the interobserver variation coefficient for measured mean LAVmax and LAVmin was 7.6%, 7.9%, respectively (Figure 5).

## DISCUSSION

In the present study, we examined whether the newly developed LAVT method can be used to evaluate LAV and provide normal LAV reference indices for evaluation of left atrial function in normal human fetuses. Left atrial function can best be characterized by pressure-volume loops, similar to methods used to estimate left ventricular function [22–23]. However, invasive methods for the determination of instantaneous left atrial pressures are required for this evaluation. In adults, CT and MRI are considered more accurately than echocardiographic methods in the quantification of LAV [12, 24]. But for fetuses, those cardiac scanning modalities are infeasible because of its inability to conduct ECG gating technology or harmful radiation effects. Thus, with the innovation of various new technologies, echocardiography has been ever widely used in screening for fetal heart diseases [2]. Several initial studies indicated the Applicability of LAVT method in assessing LAV and function has been validated in adult investigation [15, 25–26]. To the best of our knowledge, this is the first investigation attempted to quantify LAV in a relatively large group of normal fetuses.

There was an increase of up to 20-fold in fetal maximal and minimal LAV between 21 weeks and 40 weeks that increased faster during the last quarter of pregnancy. The quadratic shape of these growth curves resembles general fetal growth curves that are related to GA. However, they are different from linear growth curves that have been reported previously for M-mode diameter measurements of the left atrial size calculated from 1 dimension [27]. Manual traced left atrial areas were found correlated with GA. LAV increased with GA, which is consistent with our study [28–29]. It may add useful information to future studies of fetal LA [28–30]. Theoretically, the left atrial mechanical function consists of three phases within the cardiac cycle [31]. First, during ventricular systole and isovolumic relaxation, left atrial functions as a “reservoir” that receives blood from pulmonary venous return and stores energy in the form of pressure. Second, during the early phase of ventricular diastole, the left atrial operates as a “conduit” for transfer of blood into



the left ventricle (LV) after mitral valve opening via a pressure gradient. Third, during the late phase of ventricular diastole, LA performs as a “booster pump” through the contractile function which normally serves to augment the LV stroke volume by approximately 20% [31]. In normal adults, the TLAVCs consists of 2 peaks and 2 valleys and phased LAV can be easily distinguished [26]. However, in fetuses that would be difficult without the guide of the electrocardiogram, since E and A wave of diastolic mitral flow spectrum may fuse as a result of fast fetal heartbeat, thus the second valley become blurred in the curve (Figure 1).

In this study, as fetal electrocardiogram cannot routinely be available, phasic left atrial functions cannot be acquired from the TLAVCs. Some studies were done with speckle tracking analysis of the atria [32, 23]. In conclusion, left atrial EF was acquired through LAVmax and LAVmin obtained from the curve, and the result showed that it remained stable with advancing GA. It resembles the growing pattern of left atrial shortening fraction calculated using the formula:  $(\text{end-systolic diameter} - \text{end-diastolic diameter}) / \text{end-systolic diameter}$ , which has been demonstrated to be an alternative parameter for assessing fetal diastolic function [33]. In adults, several studies have found an association between increased ventricular filling pressure and increased LAV as well as EF, with changes in its volume correlating with an increase in risk [34–38]. LAV may be more reliable in the assessment of diastole than mitral Doppler [39]. It is a stable and reliable parameter that reflects the duration and severity of diastolic dysfunction. The study by Briguori et al. [40] in adults suggested that left ventricular diastolic function could be better assessed through left atrial motion than through mitral flows in patients with hypertrophic cardiomyopathy. Later a similar study by Zalinski et al. [41] in fetuses of women with diabetes mellitus showed that left atrial shortening was decreased as compared with that in healthy fetuses. Further studies would be needed to determine the relationship between LAV and EF and diastolic dysfunction under pathological states in fetuses.

### **Study limitations**

There were several limitations to this study. First, it was a pilot study to apply the LAVT method to the determination of LAV in normal human fetuses. LAV data obtained through this method is lack of validations in the in-vitro study or animal experiments. Thus, to approximate the true

LAV, more studies are necessary to further assess the accuracy of this method in the future. Second, phasic functions of left atrium cannot be studied for a lack of guide of fetal electrocardiogram. Third, there were several limiting factors for TLAVCs acquisition. An important limiting factor is a persistent unfavorable fetal position, which precludes the sonographers to approach the standard views, mainly the 2-chamber view, which may potentially affect the accuracy of the acquired measurements. Other limiting factors for acquisition include: low image resolution at young GA, abundant fetal movement, numerous acoustic shadows.

## **CONCLUSION**

This study presents reference ranges for indices of LAV for normal fetuses from 21 to 40 weeks of gestation. The growth curve of LAV of the normal human fetus is in line with that of left ventricular. In our opinion, more studies are needed to assess that extent measurements in fetuses in pathological states deviate from normal and whether these measurements can be of use in the prediction of fetal outcome. Although there still exists several limiting factors about the application of this method, LAVT method has proven to be a feasible method to estimate fetal LAV as well as left atrial EF during the second half of gestation, suggesting the potential value of this method in assessing left ventricular diastolic function of fetal hearts, especially under pathological conditions in mater or in fetus.

## **Supplementary material**

Supplementary material is available at [https://journals.viamedica.pl/kardiologia\\_polska](https://journals.viamedica.pl/kardiologia_polska).

**Acknowledgments:** This work was supported by Medical Health Science and Technology Project of Zhejiang Provincial Health Commission (NO.2018RC046).

**Conflict of interest:** The authors declare that they have no conflict of interest.

## REFERENCES

1. Allan LD, Crawford DC, Anderson RH, et al. Spectrum of congenital heart disease detected echocardiographically in prenatal life. *Br Heart J.* 1985; 54(5): 523–526, doi: [10.1136/hrt.54.5.523](https://doi.org/10.1136/hrt.54.5.523), indexed in Pubmed: [4052293](https://pubmed.ncbi.nlm.nih.gov/4052293/).
2. Fyfe DA, Kline CH. Fetal echocardiographic diagnosis of congenital heart disease. *Pediatr Clin North Am.* 1990; 37(1): 45–67, doi: [10.1016/s0031-3955\(16\)36831-6](https://doi.org/10.1016/s0031-3955(16)36831-6), indexed in Pubmed: [2408003](https://pubmed.ncbi.nlm.nih.gov/2408003/).
3. Silverman NH, Schmidt KG. Ventricular volume overload in the human fetus: observations from fetal echocardiography. *J Am Soc Echocardiogr.* 1990; 3(1): 20–29, doi: [10.1016/s0894-7317\(14\)80295-2](https://doi.org/10.1016/s0894-7317(14)80295-2), indexed in Pubmed: [2310588](https://pubmed.ncbi.nlm.nih.gov/2310588/).
4. Guirado L, Crispi F, Masoller N, et al. Biventricular impact of mild to moderate fetal pulmonary valve stenosis. *Ultrasound Obstet Gynecol.* 2018; 51(3): 349–356, doi: [10.1002/uog.17456](https://doi.org/10.1002/uog.17456), indexed in Pubmed: [28295792](https://pubmed.ncbi.nlm.nih.gov/28295792/).
5. Garcia-Canadilla P, Dejea H, Bonnin A, et al. Complex congenital heart disease associated with disordered myocardial architecture in a midtrimester human fetus. *Circ Cardiovasc Imaging.* 2018; 11(10): e007753, doi: [10.1161/CIRCIMAGING.118.007753](https://doi.org/10.1161/CIRCIMAGING.118.007753), indexed in Pubmed: [30354476](https://pubmed.ncbi.nlm.nih.gov/30354476/).
6. Soveral I, Crispi F, Walter C, et al. Early cardiac remodeling in aortic coarctation: insights from fetal and neonatal functional and structural assessment. *Ultrasound Obstet Gynecol.* 2020; 56(6): 837–849, doi: [10.1002/uog.21970](https://doi.org/10.1002/uog.21970), indexed in Pubmed: [31909552](https://pubmed.ncbi.nlm.nih.gov/31909552/).
7. DeVore GR, Portella PP, Andrade EH, et al. Cardiac measurements of size and shape in fetuses with absent or reversed end-diastolic velocity of the umbilical artery and perinatal survival and severe growth restriction before 34 weeks' gestation. *J Ultrasound Med.* 2021; 40(8): 1543–1554, doi: [10.1002/jum.15532](https://doi.org/10.1002/jum.15532), indexed in Pubmed: [33124711](https://pubmed.ncbi.nlm.nih.gov/33124711/).
8. Van Mieghem T, Giusca S, DeKoninck P, et al. Methods for prenatal assessment of fetal cardiac function. *Prenat Diagn.* 2009; 29(13): 1193–1203, doi: [10.1002/pd.2379](https://doi.org/10.1002/pd.2379), indexed in Pubmed: [19816885](https://pubmed.ncbi.nlm.nih.gov/19816885/).
9. Lussier EC, Yeh SJ, Chih WL, et al. Reference ranges and Z-scores for fetal cardiac measurements from two-dimensional echocardiography in Asian population. *PLoS One.* 2020; 15(6): e0233179, doi: [10.1371/journal.pone.0233179](https://doi.org/10.1371/journal.pone.0233179), indexed in Pubmed: [32584813](https://pubmed.ncbi.nlm.nih.gov/32584813/).

10. Schmidt KG, Silverman NH, Van Hare GF, et al. Two-dimensional echocardiographic determination of ventricular volumes in the fetal heart. Validation studies in fetal lambs. *Circulation*. 1990; 81(1): 325–333, doi: [10.1161/01.cir.81.1.325](https://doi.org/10.1161/01.cir.81.1.325), indexed in Pubmed: [2297836](https://pubmed.ncbi.nlm.nih.gov/2297836/).
11. DeVore GR, Klas B, Satou G, et al. Evaluation of the right and left ventricles: An integrated approach measuring the area, length, and width of the chambers in normal fetuses. *Prenat Diagn*. 2017; 37(12): 1203–1212, doi: [10.1002/pd.5166](https://doi.org/10.1002/pd.5166), indexed in Pubmed: [29023931](https://pubmed.ncbi.nlm.nih.gov/29023931/).
12. Avelar E, Durst R, Rosito GA, et al. Comparison of the accuracy of multidetector computed tomography versus two-dimensional echocardiography to measure left atrial volume. *Am J Cardiol*. 2010; 106(1): 104–109, doi: [10.1016/j.amjcard.2010.02.021](https://doi.org/10.1016/j.amjcard.2010.02.021), indexed in Pubmed: [20609656](https://pubmed.ncbi.nlm.nih.gov/20609656/).
13. Pearlman JD, Triulzi MO, King ME, et al. Left atrial dimensions in growth and development: normal limits for two-dimensional echocardiography. *J Am Coll Cardiol*. 1990; 16(5): 1168–1174, doi: [10.1016/0735-1097\(90\)90549-5](https://doi.org/10.1016/0735-1097(90)90549-5), indexed in Pubmed: [2229763](https://pubmed.ncbi.nlm.nih.gov/2229763/).
14. Gutman J, Wang YS, Wahr D, et al. Normal left atrial function determined by 2-dimensional echocardiography. *Am J Cardiol*. 1983; 51(2): 336–340, doi: [10.1016/s0002-9149\(83\)80061-7](https://doi.org/10.1016/s0002-9149(83)80061-7), indexed in Pubmed: [6823848](https://pubmed.ncbi.nlm.nih.gov/6823848/).
15. Kusunose K, Chono T, Tabata T, et al. Echocardiographic image tracker with a speckle adaptive noise reduction filter for the automatic measurement of the left atrial volume curve. *Eur Heart J Cardiovasc Imaging*. 2014; 15(5): 509–514, doi: [10.1093/ehjci/jet196](https://doi.org/10.1093/ehjci/jet196), indexed in Pubmed: [24165117](https://pubmed.ncbi.nlm.nih.gov/24165117/).
16. DeVore GR, Klas B, Satou G, et al. Evaluation of fetal left ventricular size and function using speckle-tracking and the simpson rule. *J Ultrasound Med*. 2019; 38(5): 1209–1221, doi: [10.1002/jum.14799](https://doi.org/10.1002/jum.14799), indexed in Pubmed: [30244474](https://pubmed.ncbi.nlm.nih.gov/30244474/).
17. DeVore GR, Klas B, Satou G, et al. Speckle tracking analysis to evaluate the size, shape, and function of the atrial chambers in normal fetuses at 20-40 weeks of gestation. *J Ultrasound Med*. 2022; 41(8): 2041–2057, doi: [10.1002/jum.15888](https://doi.org/10.1002/jum.15888), indexed in Pubmed: [34825711](https://pubmed.ncbi.nlm.nih.gov/34825711/).

18. Toyoda T, Baba H, Akasaka T, et al. Assessment of regional myocardial strain by a novel automated tracking system from digital image files. *J Am Soc Echocardiogr.* 2004; 17(12): 1234–1238, doi: [10.1016/j.echo.2004.07.010](https://doi.org/10.1016/j.echo.2004.07.010), indexed in Pubmed: [15562260](https://pubmed.ncbi.nlm.nih.gov/15562260/).
19. Gembruch U. Prenatal diagnosis of congenital heart disease. *Prenat Diagn.* 1997; 17(13): 1283–1298.
20. Bland JM, Altman DG. Applying the right statistics: analyses of measurement studies. *Ultrasound Obstet Gynecol.* 2003; 22(1): 85–93, doi: [10.1002/uog.122](https://doi.org/10.1002/uog.122), indexed in Pubmed: [12858311](https://pubmed.ncbi.nlm.nih.gov/12858311/).
21. Bland JM, Altman DG. Measurement error proportional to the mean. *BMJ.* 1996; 313(7049): 106, doi: [10.1136/bmj.313.7049.106](https://doi.org/10.1136/bmj.313.7049.106), indexed in Pubmed: [8688716](https://pubmed.ncbi.nlm.nih.gov/8688716/).
22. Pagel PS, Kehl F, Gare M, et al. Mechanical function of the left atrium: new insights based on analysis of pressure-volume relations and Doppler echocardiography. *Anesthesiology.* 2003; 98(4): 975–994, doi: [10.1097/00000542-200304000-00027](https://doi.org/10.1097/00000542-200304000-00027), indexed in Pubmed: [12657862](https://pubmed.ncbi.nlm.nih.gov/12657862/).
23. Payne RM, Stone HL, Engelken EJ. Atrial function during volume loading. *J Appl Physiol.* 1971; 31(3): 326–331, doi: [10.1152/jappl.1971.31.3.326](https://doi.org/10.1152/jappl.1971.31.3.326), indexed in Pubmed: [5111850](https://pubmed.ncbi.nlm.nih.gov/5111850/).
24. Keller AM, Gopal AS, King DL. Left and right atrial volume by freehand three-dimensional echocardiography: in vivo validation using magnetic resonance imaging. *Eur J Echocardiogr.* 2000; 1(1): 55–65, doi: [10.1053/euje.2000.0010](https://doi.org/10.1053/euje.2000.0010), indexed in Pubmed: [12086217](https://pubmed.ncbi.nlm.nih.gov/12086217/).
25. Gupta S, Matulevicius SA, Ayers CR, et al. Left atrial structure and function and clinical outcomes in the general population. *Eur Heart J.* 2013; 34(4): 278–285, doi: [10.1093/eurheartj/ehs188](https://doi.org/10.1093/eurheartj/ehs188), indexed in Pubmed: [22782941](https://pubmed.ncbi.nlm.nih.gov/22782941/).
26. Ogawa K, Hozumi T, Sugioka K, et al. Automated assessment of left atrial function from time-left atrial volume curves using a novel speckle tracking imaging method. *J Am Soc Echocardiogr.* 2009; 22(1): 63–69, doi: [10.1016/j.echo.2008.10.016](https://doi.org/10.1016/j.echo.2008.10.016), indexed in Pubmed: [19131004](https://pubmed.ncbi.nlm.nih.gov/19131004/).
27. Allan LD, Joseph MC, Boyd EG, et al. M-mode echocardiography in the developing human fetus. *Br Heart J.* 1982; 47(6): 573–583, doi: [10.1136/hrt.47.6.573](https://doi.org/10.1136/hrt.47.6.573), indexed in Pubmed: [7082505](https://pubmed.ncbi.nlm.nih.gov/7082505/).

28. DeVore GR, Klas B, Satou G, et al. Evaluation of fetal left ventricular size and function using speckle-tracking and the simpson rule. *J Ultrasound Med.* 2019; 38(5): 1209–1221, doi: [10.1002/jum.14799](https://doi.org/10.1002/jum.14799), indexed in Pubmed: [30244474](https://pubmed.ncbi.nlm.nih.gov/30244474/).
29. DeVore GR, Klas B, Satou G, et al. Speckle tracking analysis to evaluate the size, shape, and function of the atrial chambers in normal fetuses at 20-40 weeks of gestation. *J Ultrasound Med.* 2022; 41(8): 2041–2057, doi: [10.1002/jum.15888](https://doi.org/10.1002/jum.15888), indexed in Pubmed: [34825711](https://pubmed.ncbi.nlm.nih.gov/34825711/).
30. García-Otero L, Gómez O, Rodríguez-López M, et al. Nomograms of fetal cardiac dimensions at 18-41 weeks of gestation. *Fetal Diagn Ther.* 2020; 47(5): 387–398, doi: [10.1159/000494838](https://doi.org/10.1159/000494838), indexed in Pubmed: [30612128](https://pubmed.ncbi.nlm.nih.gov/30612128/).
31. Abhayaratna WP, Seward JB, Appleton CP, et al. Left atrial size: physiologic determinants and clinical applications. *J Am Coll Cardiol.* 2006; 47(12): 2357–2363, doi: [10.1016/j.jacc.2006.02.048](https://doi.org/10.1016/j.jacc.2006.02.048), indexed in Pubmed: [16781359](https://pubmed.ncbi.nlm.nih.gov/16781359/).
32. Meister M, Axt-Flidner R, Graupner O, et al. Atrial and ventricular deformation analysis in normal fetal hearts using two-dimensional speckle tracking echocardiography. *Fetal Diagn Ther.* 2020; 47(9): 699–710, doi: [10.1159/000508881](https://doi.org/10.1159/000508881), indexed in Pubmed: [32615558](https://pubmed.ncbi.nlm.nih.gov/32615558/).
33. Zielinsky P, Luchese S, Manica JL, et al. Left atrial shortening fraction in fetuses with and without myocardial hypertrophy in diabetic pregnancies. *Ultrasound Obstet Gynecol.* 2009; 33(2): 182–187, doi: [10.1002/uog.6154](https://doi.org/10.1002/uog.6154), indexed in Pubmed: [19012275](https://pubmed.ncbi.nlm.nih.gov/19012275/).
34. Moller JE, Hillis GS, Oh JK, et al. Left atrial volume: a powerful predictor of survival after acute myocardial infarction. *Circulation.* 2003; 107(17): 2207–2212, doi: [10.1161/01.CIR.0000066318.21784.43](https://doi.org/10.1161/01.CIR.0000066318.21784.43), indexed in Pubmed: [12695291](https://pubmed.ncbi.nlm.nih.gov/12695291/).
35. Tsang TSM, Barnes ME, Gersh BJ, et al. Left atrial volume as a morphophysiological expression of left ventricular diastolic dysfunction and relation to cardiovascular risk burden. *Am J Cardiol.* 2002; 90(12): 1284–1289, doi: [10.1016/s0002-9149\(02\)02864-3](https://doi.org/10.1016/s0002-9149(02)02864-3), indexed in Pubmed: [12480035](https://pubmed.ncbi.nlm.nih.gov/12480035/).
36. Appleton CP, Galloway JM, Gonzalez MS, et al. Estimation of left ventricular filling pressures using two-dimensional and Doppler echocardiography in adult patients with cardiac disease. Additional value of analyzing left atrial size, left atrial ejection fraction and the difference in duration of pulmonary venous and mitral flow velocity at atrial

- contraction. *J Am Coll Cardiol.* 1993; 22(7): 1972–1982, doi: [10.1016/0735-1097\(93\)90787-2](https://doi.org/10.1016/0735-1097(93)90787-2), indexed in Pubmed: [8245357](https://pubmed.ncbi.nlm.nih.gov/8245357/).
37. Sousa AC. Left atrial volume as an index of diastolic function. *Arq Bras Cardiol.* 2006; 87(3): e27–e33, doi: <https://doi.org/10.1590/S0066-782X2006001600031>.
38. Kosmala W, Marwick TH, Przewłocka-Kosmala M. Echocardiography in patients with heart failure: recent advances and future perspectives. *Kardiol Pol.* 2021; 79(1): 5–17, doi: [10.33963/KP.15720](https://doi.org/10.33963/KP.15720), indexed in Pubmed: [33394579](https://pubmed.ncbi.nlm.nih.gov/33394579/).
39. Kupczyńska K, Mandoli GE, Cameli M, et al. Left atrial strain - a current clinical perspective. *Kardiol Pol.* 2021; 79(9): 955–964, doi: [10.33963/KP.a2021.0105](https://doi.org/10.33963/KP.a2021.0105), indexed in Pubmed: [34599503](https://pubmed.ncbi.nlm.nih.gov/34599503/).
40. Briguori C, Betocchi S, Losi MA, et al. Noninvasive evaluation of left ventricular diastolic function in hypertrophic cardiomyopathy. *Am J Cardiol.* 1998; 81(2): 180–187, doi: [10.1016/s0002-9149\(97\)00870-9](https://doi.org/10.1016/s0002-9149(97)00870-9), indexed in Pubmed: [9591902](https://pubmed.ncbi.nlm.nih.gov/9591902/).
41. Zielinsky P, Satler F, Luchese S, et al. Study of global left atrial shortening in fetuses of diabetic mothers. *Arq Bras Cardiol.* 2004; 83(6): 473–5; 470, doi: [10.1590/s0066-782x2004001800005](https://doi.org/10.1590/s0066-782x2004001800005), indexed in Pubmed: [15654444](https://pubmed.ncbi.nlm.nih.gov/15654444/).

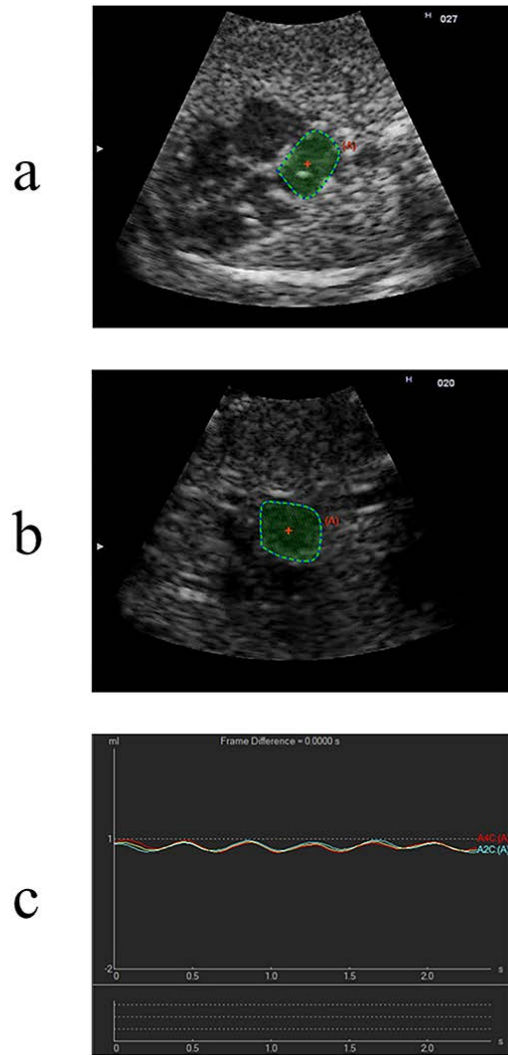


**Figure 1.** The manual trace of left atrial endocardium at the level of 4-chamber (A) and 2-chamber (B) view at first frame of the dynamic images. Time-left atrial volume curves (C) were automatically obtained with left atrial tracking method, which contained the volume corresponding to each frame, including volume of 4-chamber view (the red curve), 2-chamber view (the blue curve) as well as the overall volume (the yellow curve) by biplane Simpson's rule



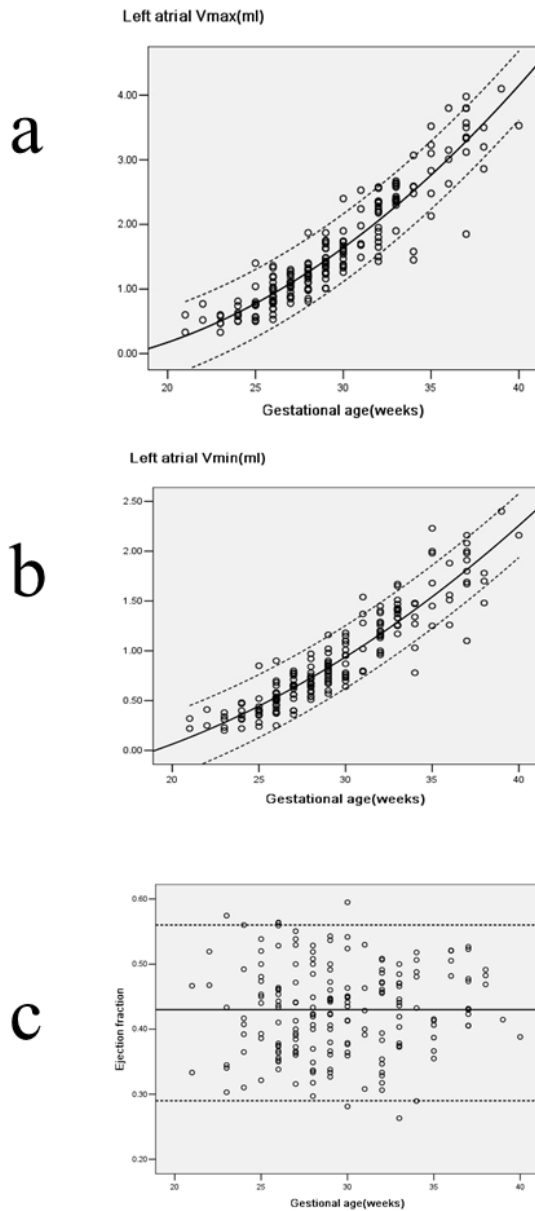


**Figure 2.** Volume measurements of left atrium and ejection fraction plotted against gestational age. Atria volume showed a consistently stronger correlation than that found with biparietal diameter (BPD). Solid lines represent the mean; dashed lines represent 5% and 95% confidence

interval (CI). **A.** Left atrial maximal volume. **B.** Left atrial minimal volume. **C.** Left atrial ejection fraction

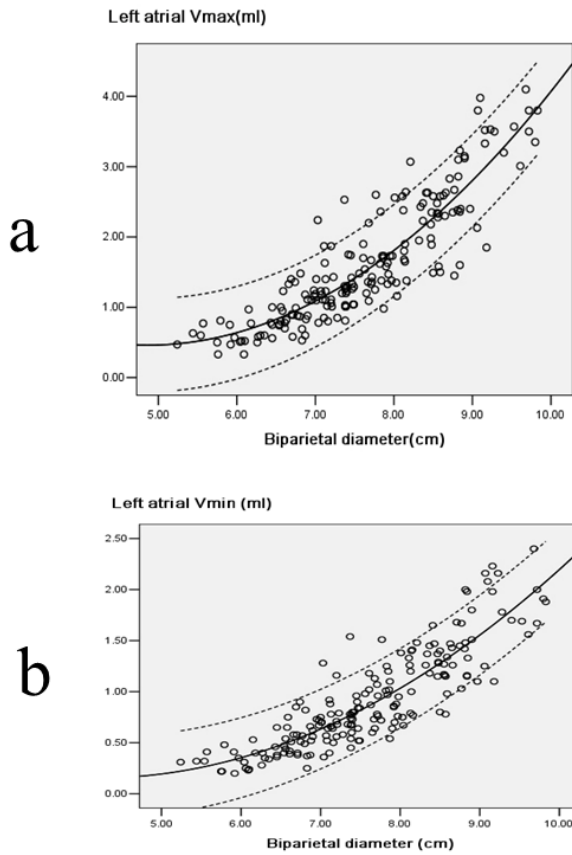


**Figure 3.** Volume measurements of left atrium plotted against biparietal diameter (BPD). Solid lines represent the mean; dashed lines represent 5% and 95% confidence interval. **A** Left atrial maximal volume. **B.** Left atrial minimal volume

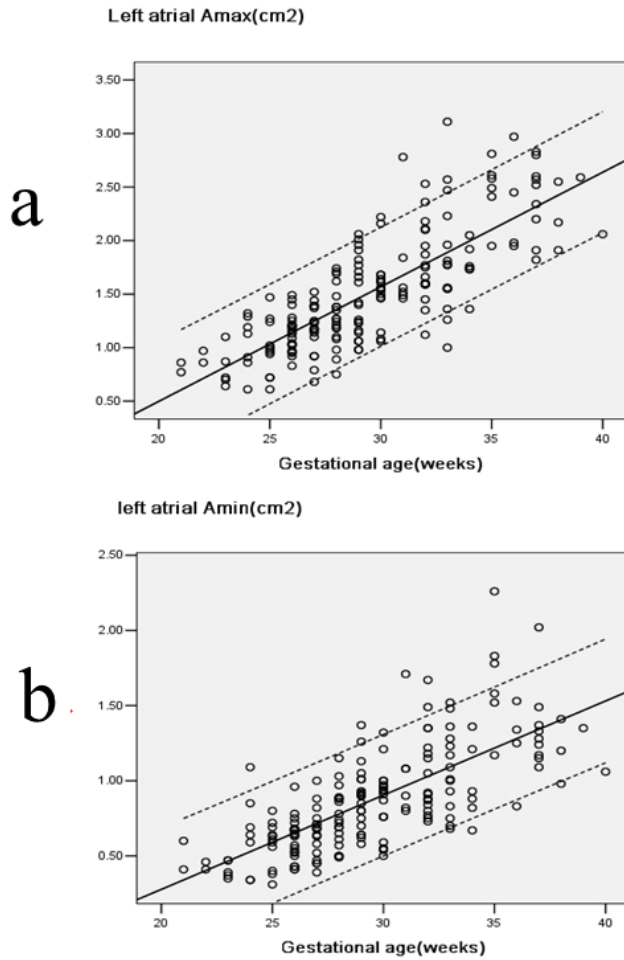
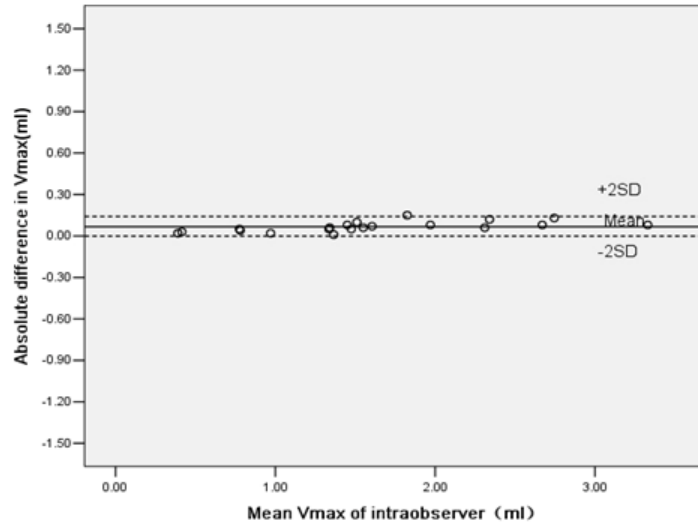


**Figure 4.** Area measurements of left atrium plotted against gestational age. Solid lines represent the mean; dashed lines represent 5% and 95% confidence interval. **A.** Left atrial maximal area. **B.** Left atrial minimal area

a



b

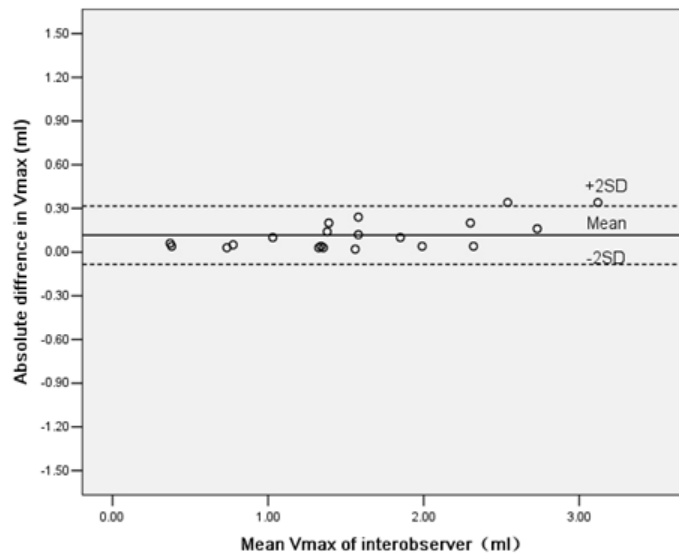


**Figure 5.** Bland-Altman plots of the absolute difference and 95% limits of agreement between paired measurements of the left atrial Vmax by the same sonographer (**A**) and two separate sonographers (**B**)